UNDULATING PROPULSION SYSTEM DESIGN

Rodríguez, J.D.

González, P.B.

Couce, A.

González, G.

Research Group INNOVACIÓNS MARIÑAS (University of A Coruña)

Abstract

Throughout history the practical implementation of propulsion mechanisms in the fluid environment based on the rotation has been easier to deal because of the state of the art in its time, and this has meant that it has not been more interest a further development of wave based mechanisms which are most of those seen in nature.

The Research Group Innovacións Mariñas, attached to the Ship Building Department. (University of A Coruña) is currently developing a wave propeller prototype (based on a invention whose antecedent can be found in invention patent nr. 200002012, author Primitivo B. Gonzalez), applicable to systems and bodies located in fluid environment, and based on the way chosen by first living organisms to move.

We are currently finishing the construction of a prototype for trials in a testing tank, whose virtual model has been developed with SOLID EDGE V.18 and its components calculated with the help of finite element module that incorporates this software. Simulation of the propeller performance has been done through software FLUENT 6.3

Keywords: Marine propeller, undulating propulsion

1. Introduction

For millions of years fish have developed skills in their displacement by water, in many ways far superior to those achieved today by technology and science of navigation. Fish instinctively use their hydrodynamic shape to exploit the principles of fluid mechanics in such a way that ship design engineers currently ship only can achieve to dream, achieving extraordinary efficiencies in its propulsion, acceleration and manoeuvrability.

For much of the last century and more intensely since the early eighties, a large number of research groups from universities in Europe and the United States have invested significant resources in investigating ways of biologically inspired marine propulsion.

During those years at the University of A Coruña (Dept. Construccions Navais - Escola Universitaria Politécnica de Ferrol) has also been initiatives in this direction (Sargo Project) with a relative success given the limited available resources.

A prototype propeller was built that uses as a means of propulsion, a flexible membrane, articulated by a series of metal rods as a skeleton. Rods are operated through a eccentrics shaft who is receiving a torque through induction electric motor drived by frequency inverter.

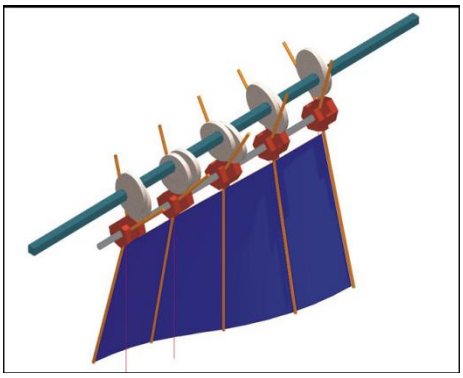

Fig.: 1. Operating principle of 1st prototype

Fig.: 2. Image of 1st Prototype

As shown in pictures, this first prototype generates an undulating surface similar to that caused by a generatrix, whose top follows a straight direction while the lower moves on a sinusoidal form.

In 2002 was obtained an invention patent: UNDULANT PROPULSION SYSTEM (ref: 200002012)

Continuing of these studies led to a doctoral thesis and to the application, (in 2005) of a second invention patent.

Subsequently was obtained a grant from the Galician Government to build a second prototype (Project: UNDULANT PROPULSION SYSTEM. COD. PGIDIT06DPI172PR8, PRINCIPAL INVESTIGATOR: PRIMITIVO B. GONZALEZ LOPEZ) which is currently under consideration. This prototype generates an undulating surface similar to that caused by a horizontal generatrix moving parallel to itself on a sinusoidal form.

In year 2008 was applicated for a third invention patent from conclusions obtained in the development of new prototype.

This communication is to reflect a part of the design process of the prototype.

It should also be noted that the European Technology Platform for Shipping: WATERBORNE considers in its Strategic Development Agenda (Annex 2, pt. 2.2.2.1) that "*Significant increases in efficiency will require more complex propulsor configurations or radical new concepts such as biomechanical designs....*"

2. Design of the new prototype

2.1 Design of mechanism driving the membrane

It aims to generate a sinusoidal waveform in a membrane through the activation of a articulated rigid structure that will support it.

To simplify our modelling, the fin (wavy shaped) is divided into a specific number of servings flat membrane (membrane segments).

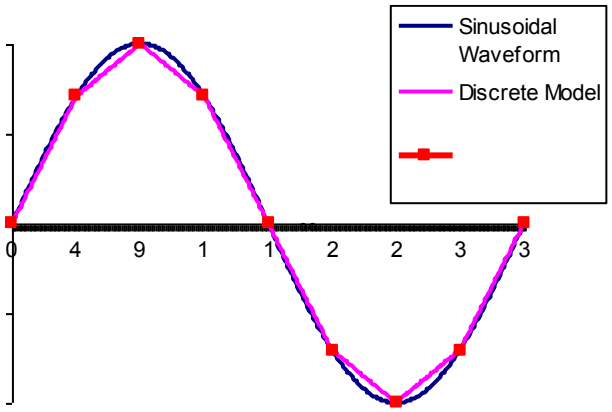

Fig.: 3. Discrete model of a sinusoidal waveform obtained through a series of straight segments that join points every 45 º

The membrane is designed in such a way that each segment is a flat shape that joins two consecutive horizontal axes, it also allows the change in distance between each pair of axes while they oscillate

In the current state of research, the mechanical model of undulatory fin is achieved through a mechanism of one degree of freedom. Motion is generated by means the mechanical torque delivered by an electrical motor connected to a frequency inverter.

Each segment is driven by two pairs of vertical pins, so that each pair of pins working on phase transmitted a vertical harmonic linear motion to a horizontal bar and two horizontal bars make up the physical support of a segment of membrane

Each "thorn", set horizontally, moves through a pair of vertical pins and each pair of pins is driven by a crank-slider system.

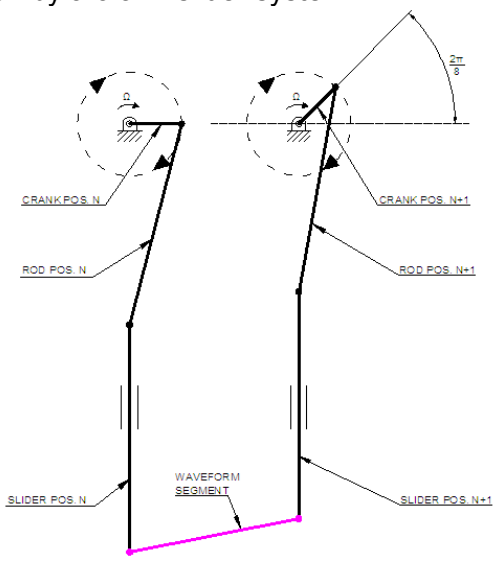

Fig.: 4. Drive scheme of a waveform segment operated through two crank-slider systems

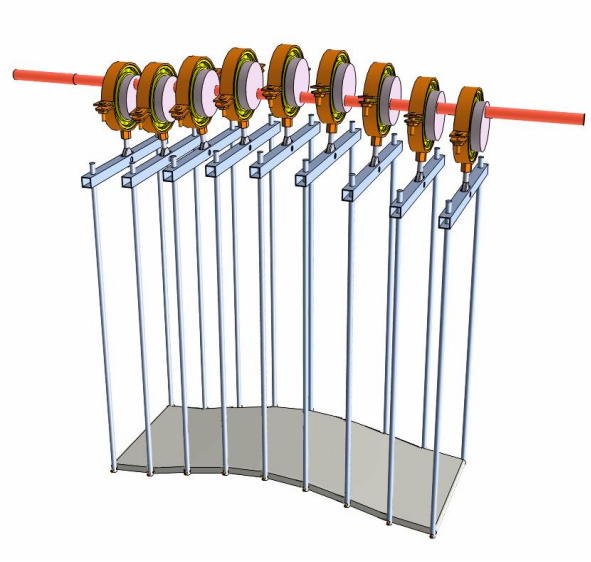

Fig.: 5. Chosen solution for the articulation of a membrane

Each segment performs a harmonic movement up and down (heave) with the amplitude of its center point and the frequency imposed by the rotation speed of the crankshaft, and a second harmonic swing motion (pitch) of a certain amplitude (depending on various parameters) and frequency imposed by the rotation speed of the crankshaft.

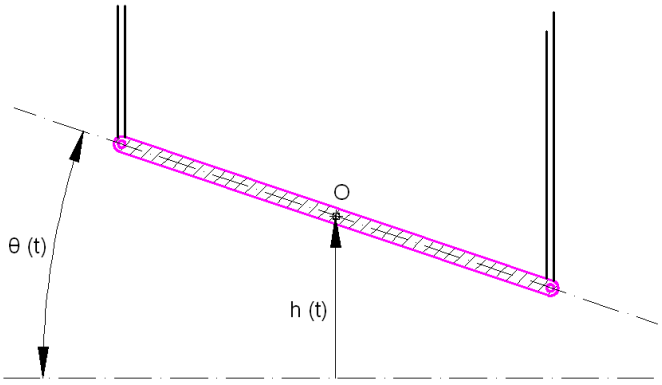

Fig.: 6. Definition of main parameters of motion: heave h (t) and θ pitch (t) for an oscillating segment

3. Methodology

Kinematical analysis of the behaviour of a waveform segment is exposed, function of several parameters: length of rods, number of segments, and so on

In order to study the motion of a waveform segment, it is modelled the drive mechanism through a double crank-slider four bar linkage.

3.1 Expression of the position and the length of the 'waveform segment' in the double crank-slider four bar linkage, 1 d.o.f.

3.1.1 Expression of the position of the slide in the crank-slider four-bar linkage without offset

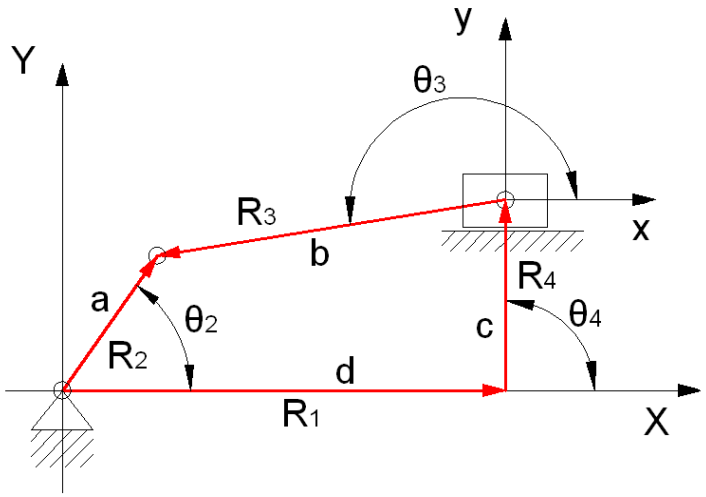

Fig.: 7. Position vectors loop for a crank - Slider four-bar linkage

The linkage to be considered can be represented by only three position vectors: $\mathbf{R_1}$, $\mathbf{R_2}$ and $\mathbf{R_3}$. (Offset vanishes because of the absence of R_4)

$\mathbf{R_1}$, variable module and constant direction vector, represents the position of the slide.

$\mathbf{R_3}$, position vector of the coupler, lies with its origin on the slide and thus defines its angle θ_3 by means of point B. This particular position of vectors leds to a vectorial loop equation:

$$\vec{R}_2 - \vec{R}_3 - \vec{R}_1 = 0 \quad (1)$$

If modules of the vectors (link lengths) are represented by symbols: a, b, c, as indicated, vectors can be replaced by equivalent complex numbers:

$$ae^{j\theta 2} - be^{j\theta 3} - de^{j\theta 1} = 0 \quad (2)$$

Introducing in (2) Euler equivalents and separating real and imaginary components:

$$\text{real component:} \quad a\cos\theta_2 - b\cos\theta_3 - d = 0 \quad (3)$$

$$\text{imaginary component:} \quad a\sin\theta_2 - b\sin\theta_3 = 0 \quad (4)$$

Equations are solved in order to determinate unknown link length: d, corresponding to the slider position function as a function of the crank position angle: θ_2. So:

$$\theta_3 = -\arcsin\left((a/b)\sin\theta_2\right) + \pi \quad (5)$$

$$d = a\cos\theta_2 - b\cos\theta_3 \quad (6)$$

3.1.2 Expressions of the position and length of the 'waveform segment' in the double crank-slider four bar linkage, *1 d.o.f.*

The phase angle between two consecutive cranks is named with the symbol 'α'. Easily can be deduced that α = 360/(n-1). Where **'n'** is the number of cranks of the transmission mechanism.

The distance between two consecutive cranks is named with the symbol 'x'.

Regarding to (5) and (6) equations. For the first slider:

$$d_1 = a\cos\theta_2 - b\cos\theta_{3,1} \quad (7)$$

$$\text{and} \quad \theta_{3,1} = -\arcsin\left((a/b)\sin\theta_2\right) + \pi \quad (8)$$

For the second slider, drived by a crank with a gap of α degree with respect to previous one:

$$d_2 = a\cos(\theta_2 - \alpha) - b\cos\theta_{3,2} \quad (9)$$

$$\text{and} \quad \theta_{3,2} = -\arcsin\left((a/b)\sin(\theta_2 - \alpha)\right) + \pi \quad (10)$$

- **'γ'** value of the angle between the 'waveform segment' under study and the horizontal plane (**pitch**)

So, for **γ** is obtained the expression:

$$\boldsymbol{\gamma = \text{arc tg}\left[(d_1 - d_2)/x\right]} \quad (11)$$

Representing the curves $\boldsymbol{\gamma(\theta_2)}$ (fig. 8), which relates the shaft advance angle with the angle between the 'waveform segment' under study and the horizontal plane for several rod length values (b), can be observed that: the longer is the rod the more similar is the curve to a sinusoidal form and so the smoother is the oscillating movement of the segment.

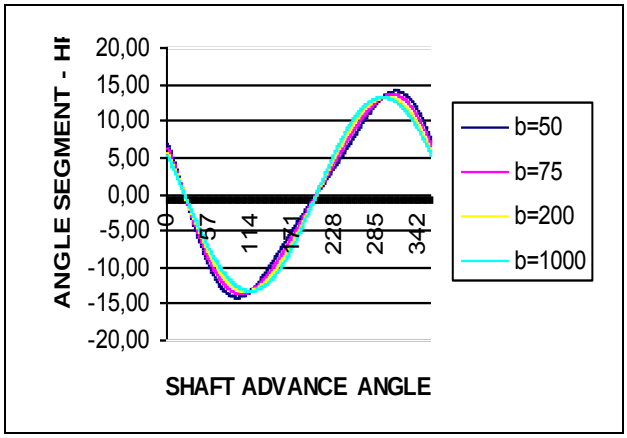

Fig.: 8. Position of the waveform segment (pitch) as a function of the shaft advance angle for several rod length values. (a=20 mm, n = 8 segments, λ = 520 mm)

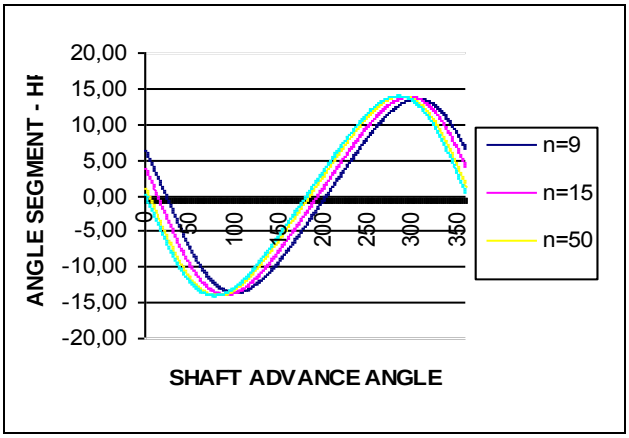

Fig.: 9. Position of the waveform segment (pitch) as a function of the shaft advance angle for several values of the number of segments. (a=20 mm, b = 75 mm, λ = 520 mm)

Also, from fig. 9 is possible to conclude that the increasing of the number of waveform segments, keeping invariable the wavelength, crank length and rod length does not involve significant changes in the evolution of the position.

- **đ:** value (mm) of the position of the segment under study in its vertical movement (**heave**)

$$\text{đ} = (d_1 + d_2) / 2 \qquad (12)$$

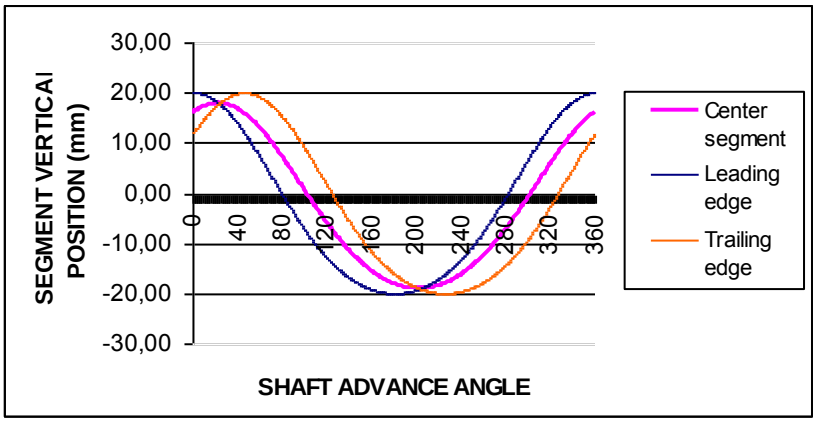

Fig.: 10. Position of the waveform segment (heave) as a function of the shaft advance angle for a rod length: b=20 mm)

Representing motion curves of the waveform segment in the same graph (fig. 11) can be observed that there is a gap between both of them. By calculations can be yielded a value close to 90º.

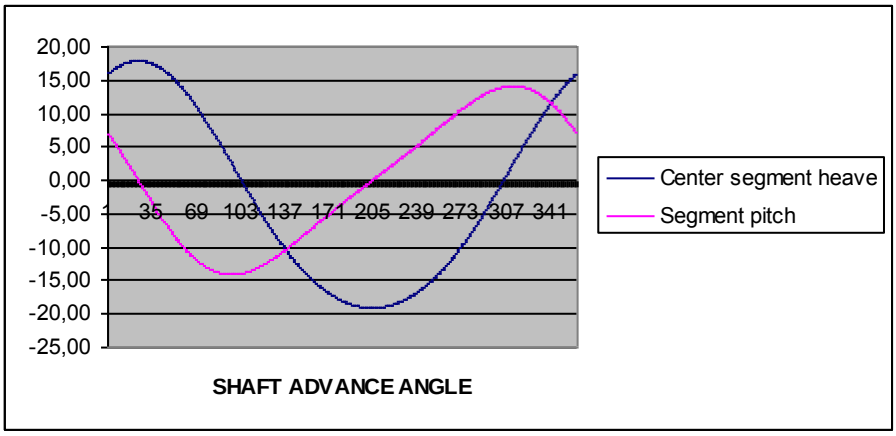

Fig.: 11. Gap between pitch and heave movements for a waveform segment.

- **'δ':** length value of the wavelength segment under review:

$$\delta = [(d_1 - d_2)^2 + x^2]^{1/2} \qquad (13)$$

Representing in fig. 12 the curves δ (θ_2) for several values of b (rod length) can be observed that as the length increases, the increasing of the length of the waveform segment decreases tending asymptotically to some value. It also notes that in a full rotation of the shaft of the mechanism each segment of waveform undergoes two elongations.

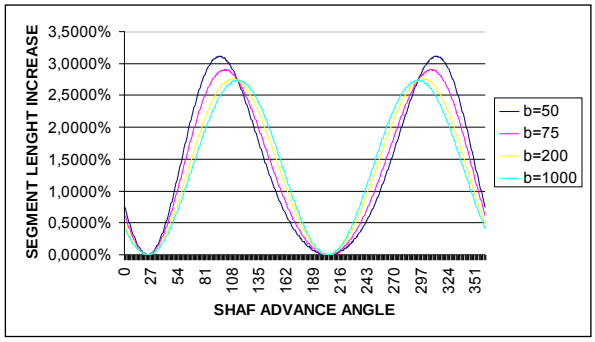

Fig.: 12. Increasing of the length of the waveform segment as a function of the shaft progress angle for several rod length values. (a=20 mm, n = 8 segments, λ = 520 mm)

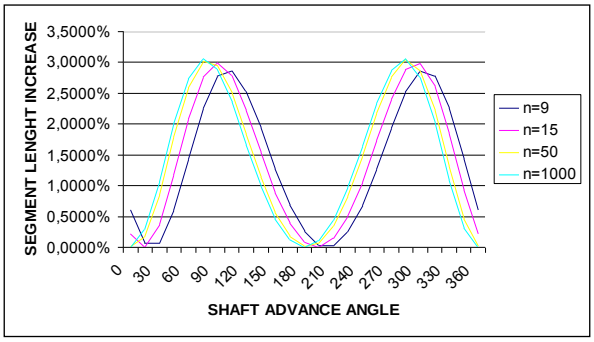

Fig.: 13. Increasing of the length of the waveform segment as a function of the shaft progress angle for several segment number values. (a=20 mm, b = 75 mm, λ = 520 mm)

Representing the curve δ (θ_2) as a function of several values of n (fig. 13) (number of waveform segments) can be observed that, as the number of segments increases the segment relative length of the segment increases tending asymptotically to some value.

3.2 Expression of the angular velocity of a waveform segment drived by two sliders with eighth of period gap between them.

3.2.1 Expression of the slider velocity in the crank slider four bar linkage without *offset*

Vectorial loop equation obtained above:

$$ae^{j\theta 2} - be^{j\theta 3} - de^{j\theta 1} = 0 \qquad (14)$$

Derivating the expression (14) with respect to time, keeping invariable: a, b, θ_1:

$$ja\omega_2 e^{j\theta 2} - jb\omega_3 e^{j\theta 3} - d' = 0 \qquad (15)$$

The value named: d' is the lineal velocity of the slider. Introducing Euler equivalents in the equation (15) ad separating real and imaginary parts:

Real part (x-axe component):

$$-a\omega_2 \sin\theta_2 + b\omega_3 \sin\theta_3 - d' = 0 \qquad (16)$$

Imaginary part (y-axe component):

$$a\omega_2 \cos\theta_2 - b\omega_3 \cos\theta_3 = 0 \qquad (17)$$

Solving the equation system (16), (17):

$$\omega_3 = (a\cos\theta_2 / b\cos\theta_3)\,\omega_2 \qquad (18)$$

$$d' = -a\omega_2 \sin\theta_2 + b\omega_3 \sin\theta_3 \qquad (19)$$

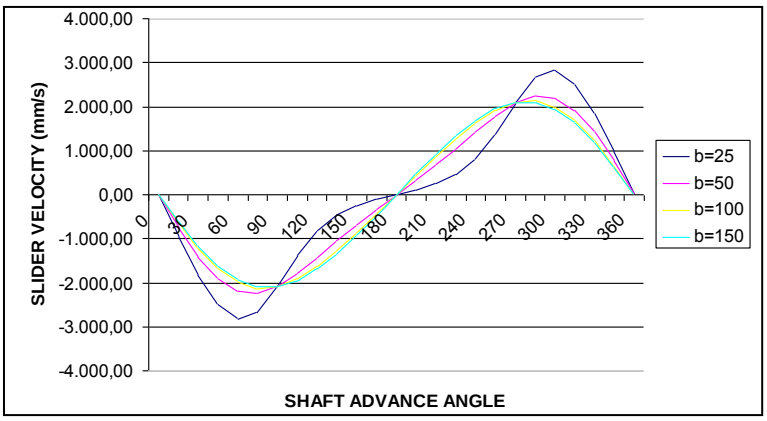

Fig.: 14. Slider instantaneous velocity as a function of the shaft progress angle for several values of rod length (a=20 mm, n = 8 segments, λ = 520 mm, ω=1000 rpm)

3.2.2 Expression of the slider acceleration in the crank slider four bar linkage without *offset*

From the above obtained velocity equation:

$$ja\omega_2 e^{j\theta 2} - jb\omega_3 e^{j\theta 3} - d' = 0 \qquad (15)$$

Derivating the expression in order to obtain acceleration equation and eliminating j^2, then:

$$(a\alpha_2 j e^{j\theta 2} - a\omega_2^2 e^{j\theta 2}) - (b\alpha_3 j e^{j\theta 3} - b\omega_3^2 e^{j\theta 3}) - d'' = 0 \qquad (20)$$

The two unknown parameters in equation (20) are: angular acceleration of link 3, that is: α_3 and linear acceleration of the slider: d". In order to solve this equation system, Euler equivalents are introduced and real and imaginary parts are separated.

Real part.

$$-a\alpha_2 \operatorname{sen}\theta_2 - a\omega_2^2 \cos\theta_2 + b\alpha_3 \operatorname{sen}\theta_3 + b\omega_3^2 \cos\theta_3 - d'' = 0 \qquad (21)$$

Imaginary part.

$$a\alpha_2 \cos\theta_2 - a\omega_2^2 \operatorname{sen}\theta_2 - b\alpha_3 \cos\theta_3 + b\omega_3^2 \cos\theta_3 = 0 \qquad (22)$$

Solving the equation system (21), (22):

$$\boldsymbol{\alpha_3} = (a\alpha_2 \cos\theta_2 - a\omega_2^2 \operatorname{sen}\theta_2 + b\omega_3^2 \cos\theta_3) / b\cos\theta_3 \qquad (23)$$

$$d'' = -a\alpha_2 \operatorname{sen}\theta_2 - a\omega_2^2 \cos\theta_2 + b\alpha_3 \operatorname{sen}\theta_3 + b\omega_3^2 \cos\theta_3 \qquad (24)$$

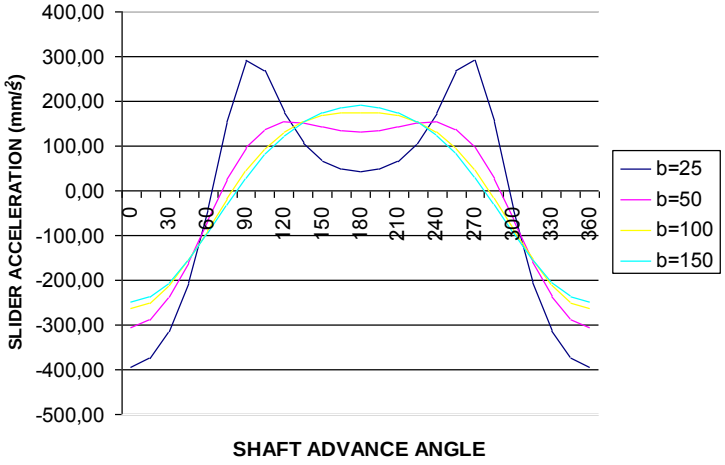

Fig.: 15. Slider acceleration as a function of the shaft progress angle for several rod lengths. (a=20 mm, n = 8 segment, λ = 520 mm, ω=1000 rpm)

3.2.3. Expression of the angular velocity of a waveform segment drived by two sliders with eight of period gap between them.

$$\gamma = \text{arc tg}\,[(d_1 - d_2) / x] \qquad (11)$$

Derivating with respect to t and replacing d'(θ) and d''(θ) by their expressions, then:

$$\gamma' = \frac{-(a/x)\,\omega\,\operatorname{sen}\theta_{21} + (b/x)\,\operatorname{sen}\theta_{31}\,\theta'_{31} + (a/x)\,\omega\,\operatorname{sen}\theta_{22} - (b/x)\,\operatorname{sen}\theta_{32}\,\theta'_{32}}{1 + \left(\left((a\cos\theta_{21} - b\cos\theta_{31}) - (a\cos\theta_{22} - b\cos\theta_{32})\right) / x\right)^2} \qquad (25)$$

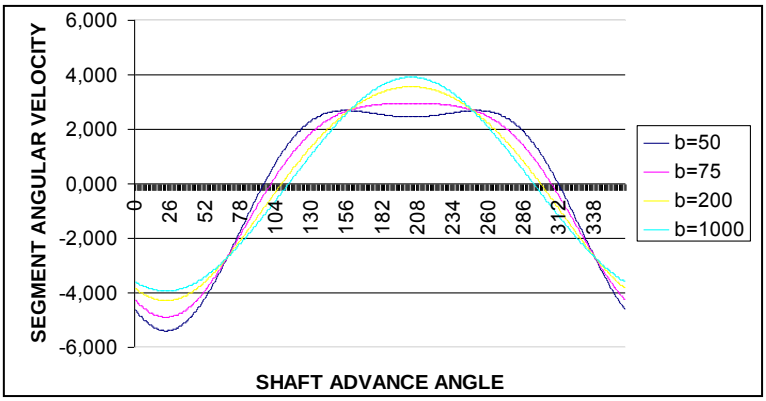

Fig.: 16. Angular velocity of a segment as a function of the shaft advance angle for several rod length values. (a=20 mm, n = 8 segments, λ = 520 mm, ω=1000 rpm)

3.3 Expression of the angular acceleration of a waveform segment drived by two sliders with eighth of period gap between them.

The numerator of the above expression is named f(θ), the denominator is named g(θ) and then the expression:

$$((a \cos \theta_{21} - b \cos\theta_{31}) - (a \cos \theta_{22} - b \cos\theta_{32})) / x = g_1(\theta) \qquad (26)$$

Derivating the numerator of the expression (25):

$$f'(\theta) = - (a/x)\, \omega^2 \cos\theta_{21} + (b/x) (\cos\theta_{31}\, \theta'^2_{31} + \operatorname{sen}\theta_{31}\, \theta''_{31}) + (a/x)\, \omega^2 \cos\theta_{22} -$$

$$- (b/x) (\cos\theta_{32}\, \theta'^2_{32} + \operatorname{sen}\theta_{32}\, \theta''_{32}) \qquad (27)$$

$$g(\theta) = 2\, f(\theta)\, g_1(\theta) \qquad (28)$$

Then, derivating the expression (25) and introducing the expressions (26), (27) y (28):

$$\gamma'' = (f'(\theta)\, g(\theta) - 2\, f^2(\theta)\, g_1(\theta)) / g^2(\theta) \qquad (29)$$

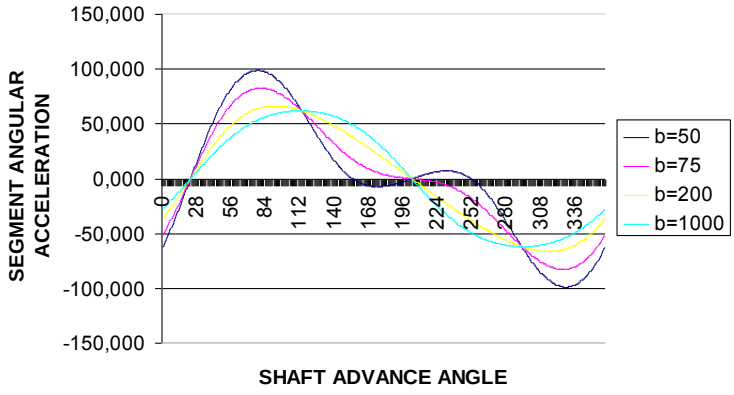

Fig.: 17. Angular acceleration of a segment as a function of the shaft advance angle for several rod length values. (a=20 mm, n = 8 segments, λ = 520 mm, ω=1000 rpm)

4. Conclusions

It has been decided to build a mechanical drive in order to generate the undulating surface over other options such as: with an electromagnetic drive, with stepper motors, including the use of electro active polymers since our focus is to study the propulsive performance of the surface that generates a waveform

From previous experience with the prototype we draw the conclusion that the transmission system by means of cams is not efficient. Therefore we decided to build an eccentric shaft by inserting a ball radial bearing between disc and collar in order to reduce friction losses.

We reject the construction of a crankshaft of an engine similar to explosion due to construction difficulties that entailed.

Kinematical analyses of the mechanism draw the conclusion of the desirability of as many segments of the wave and the maximum length of the cranks.

The chosen type of mechanism will impose a reduced length of cranks (distance between the center of eccentric shaft and the center of the eccentric disk), since the increase of this distance implies an increase in the diameter of the eccentric disc and therefore the diameter of the bearing intermediate and thus its width, weight, etc So the engine is designed for crank length of 20 or 25 mm (thus giving rise to a wave amplitude of 40 or 50 mm.

It was decided to build the undulating surface from a series of rigid segments properly designed, avoiding the use of an elongated elastic material which can be stretched when it is working, once it emerges from this analysis that each waveform segment stretches twice per shaft revolution.

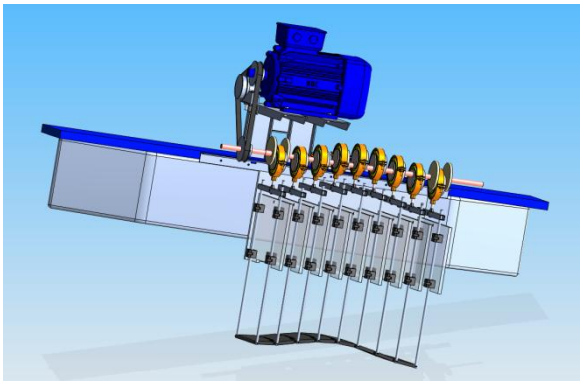

Fig.: 18. Undulating surface detail and movement conversion system

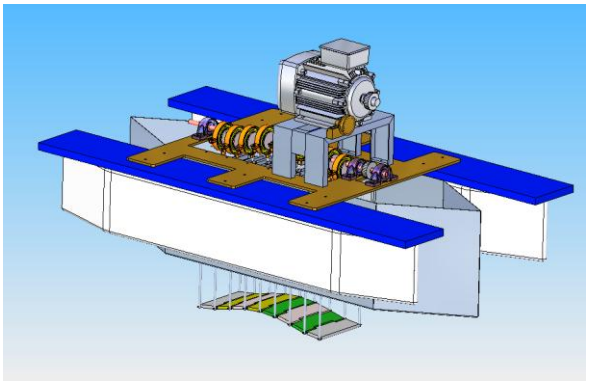

Fig.: 19. Image of the platform designed for testing the propellant surface

Bibliography

Arthur G. Erdman - George N. Sandor "Diseño de Mecanismos. Analisis y Síntesis", Ed Pearson

F.S. Hover, Ø. Haugsdal and M.S. Triantafyllou "*Control of angle of attack profiles in flapping foil propulsion."*, Journal of Fluids and Structures, accepted 2003.

H. Yamaguchi, N. Bose "*Oscillating Foils for Marine Propulsion",* Proceedings of the Fourth International Offshore and Polar Engineering Conference, Vol. 3, pp.539-544, 1994.

K. H. LOW, A. WILLY "Biomimetic Motion Planning of an Undulating Robotic Fish Fin", J*ournal of Vibration and Control* 2006; 12; 1337

M.J. Lighthill "Aquatic animal propulsion of high hydromechanical efficiency", J. Fluid Mech., Vol. 44, pp.265-301, 1970

Read, D.A., F.S. Hover, and M.S. Triantafyllou "Forces on oscillating foils for propulsion and maneuvering", Journal of Fluids and Structures 17(January):163-183

Stafiotakis M, Lane D M, Davies B C "Review of fish swimming modes for aquatic locomotion", IEEE Journal of Oceanic Engineering, vol 24, nº2

Triantafyllou, Michael S., Triantafyllou, George S. "An efficient swimming machine" Scientific American; Mar95, Vol. 272 Issue 3, p64, 7p, 1 chart, 3 diagrams, 4c

WATERBORNE Implementation Route Map (WIRM) 2007. http://www.waterborne-tp.org/

Contacts

Juan de Dios Rodríguez García
Grupo Investigación INNOVACIÓNS MARIÑAS
UNIVERSIDADE A CORUÑA
Escola Universitaria Politécnica
Avda. 19 feb. s/n
15405 FERROL
Phone: +34 981 337 400 Ext 3002 / 3081
Fax: + 34 981 337 401
E-mail : jdedios@cdf.udc.es